INSA INSTITUT NATIONAL DES SCIENCES APPLIQUÉES TOULOUSE

Jet Propulsion Laboratory
California Institute of Technology

STUDY OF ICE CRYSTALLIZATION

End of study internship

REMI CARESCHE
Department of mechanical engineering INSA Toulouse
System engineering
Presented on September 24, 2024

NASA JPL Mentor: Dr. Ellen CZAPLINSKI, Dr. Robert HODYSS
INSA Toulouse Mentor: Dr. Lucien BALDAS

2024-2025

Contents

1 Acknowledgment

I would like to express my deepest gratitude to everyone who contributed to the success of my internship at the NASA Jet Propulsion Laboratory (JPL). I am especially thankful to my mentors, Dr. Ellen Czaplinski and Dr. Robert Hodyss, for their exceptional guidance, patience, and support throughout this experience. Their expertise and advice have been invaluable to my personal and professional development.

I would also like to extend my thanks to my entire team at JPL, particularly Dr. Edith Fayolle, Dr. Bjorn Davidsson, and Dr. Ahmed Mahjoub, for their availability, and willingness to share their knowledge. Their collaboration greatly enriched my research experience.

Lastly, I want to express my appreciation to all the other interns at JPL with whom I shared this journey.

This research was carried out at the Jet Propulsion Laboratory, California Institute of Technology, and was sponsored by the JPL Visiting Student Research Program and the National Aeronautics and Space Administration (80NM0018D0004).

2 Abstract

During my six-month internship at NASA's Jet Propulsion Laboratory (JPL), I conducted research on the sublimation and crystallization processes of cometary ices, focusing on the interactions between CO and CO_2. My work involved using advanced techniques such as Fourier-transform infrared (FTIR) spectroscopy and a quartz crystal microbalance (QCM) to study these processes. The results provide us insights on the thermodynamic and kinetic behaviors of cometary ices, which are relevant for interpreting data from missions like ESA's Rosetta-Philae. Additionally, I assembled the Low-Energy Electron Diffraction (LEED) instrument for surface analysis of various ices.

3 Introduction

During my six-month internship at NASA's Jet Propulsion Laboratory (JPL) in California, I engaged in research focused on understanding the sublimation and crystallization processes of cometary ices. My work primarily involved using advanced spectroscopic techniques to characterize these processes and contributing data to the field of planetary science.

The initial phase of my internship involved setting up and assembling the Low-Energy Electron Diffraction (LEED) instrument. The goal was to equip the laboratory with an instrument capable of observing the surfaces of various ices at extremely low temperatures, enabling structural analysis.

Subsequently, I shifted my focus to the study of comets, where I utilized the Fourier-transform infrared (FTIR) spectroscopy, integrated into LEFTY (setup name), to observe the amorphous-to-crystalline transitions of water, CO_2, and CO/CO_2 ices. In addition to these crystallization studies, I used LEFTY and a quartz crystal microbalance (QCM) setup, KOALA (setup name), to measure the sublimation rates of CO from a CO/CO_2 ice mixture. These instruments provided data on the interactions between CO and CO_2 during sublimation at perihelion (closest point to the sun in the orbit).

The findings from these experiments are useful for improving our understanding of the thermodynamic and kinetic behaviors of cometary ices. These insights are relevant for interpreting data from space missions like the European Space Agency's Rosetta-Philae mission, which detected CO trapped in amorphous CO_2 phases on comet 67P/Churyumov-Gerasimenko.

4 Jet Propulsion Laboratory

The NASA Jet Propulsion Laboratory (JPL) is a federally funded research and development center located in Pasadena, California. Managed by the California Institute of Technology (Caltech), JPL is renowned for its pioneering work in robotic space exploration, Earth science, and space communication. Established in the 1930s, JPL has grown to become one of the most significant institutions in the world for advancing space technology and scientific knowledge. The laboratory's motto, "Dare Mighty Things," reflects its commitment to pushing the boundaries of what is possible in space exploration.

4.1 Historical background

JPL's origins can be traced back to the 1930s when a group of Caltech students began experimenting with rocket technology in the Arroyo Seco area of Pasadena. These early experiments laid the groundwork for the development of rocket propulsion technology.

In 1943, the group formed the Jet Propulsion Laboratory to support the U.S. Army's missile development program during World War II. JPL's early contributions to missile technology included the development of the WAC Corporal, the first American rocket to reach the edge of space.

After the war, JPL transitioned from military projects to space exploration. In 1958, JPL became a part of the newly formed NASA and launched the United States' first satellite, Explorer 1, marking the beginning of the space age. Since then, JPL has been at the forefront of numerous groundbreaking missions, including the Mariner, Viking, Voyager, and Galileo missions.

Figure 1: Explorer 1 *S*ource: JPL [a]

4.2 Organizational structure

JPL's organizational structure is designed to support its diverse array of projects and missions. The laboratory is divided into two scientific entities, each responsible for different aspects of its operations:

- Science and Technology Directorate: This directorate focuses on advancing scientific research and developing new technologies for space exploration. It includes divisions

such as the Earth Science and Technology Directorate, the Astrophysics and Space Sciences Directorate, and the Planetary Science Directorate.

- Engineering and Science Directorate: This directorate is responsible for the design, development, and testing of spacecraft and instruments. It encompasses divisions such as the Flight Projects Directorate, the Instruments and Science Data Systems Directorate, and the Mechanical Systems Engineering and Research Directorate.

4.2.1 Planetary science section

During this internship, I was assigned to the laboratory studies group within the planetary science section. This group consists of about twenty researchers. The research associated with this group is quite varied, ranging from the study of glacial structures to sublimation, the study of organic molecules, and atmospheric studies. The main idea of this group is to support the research of numerical models with concrete data, verify the data obtained from ongoing missions (such as Cassini and Rosetta-Philae), and help design instruments for missions like SHERLOK and MOXIE, two instruments installed on the Perseverance rover.

4.3 Notable missions and achievements

JPL has been at the helm of some of the most iconic and successful space missions in history. A few notable missions include:

- Voyager Missions: Launched in 1977, Voyager 1 and Voyager 2 have provided unprecedented data on the outer planets and continue to send information from beyond the solar system.
- Mars Rovers: From the Sojourner rover in 1997 to the more recent Curiosity and Perseverance rovers, JPL has revolutionized our understanding of Mars through its innovative rover missions.
- Cassini-Huygens Mission: A collaboration among NASA, ESA, and ASI, the Cassini mission to Saturn delivered breathtaking images and valuable scientific data, including the successful landing of the Huygens lander on Titan.

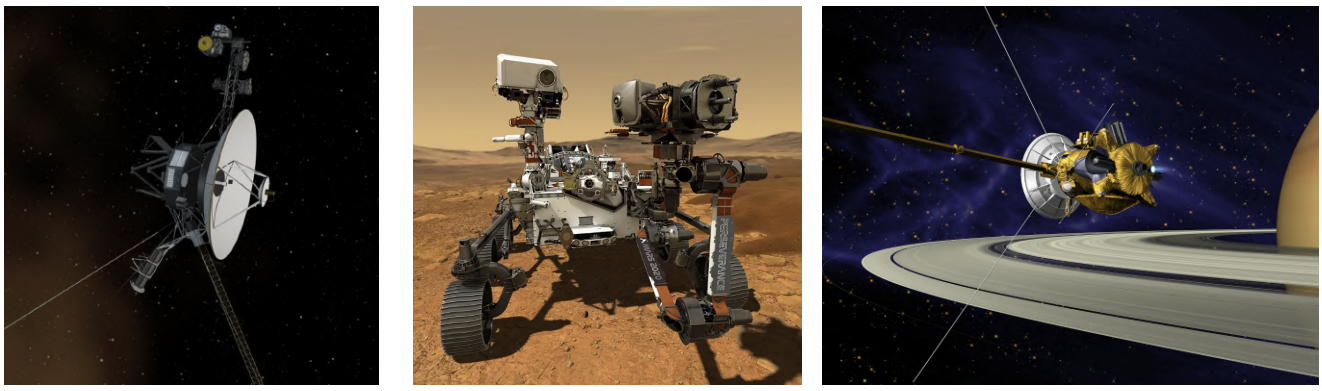

(a) Voyager 1 Spacecraft (b) Perseverance Rover (c) Cassini Spacecraft

Figure 2: JPL missions *S*ources: NASA, JPL [b], Wikipedia [a]

4.4 Future directions

The planned Mars Sample Return (MSR) campaign, a highly ambitious and collaborative effort between NASA and ESA seeking to bring Martian samples back to Earth, is preparing to undergo significant changes. Due to escalating costs and technical challenges, NASA announced its intent to revise the baseline MSR architecture, aimed at streamlining operations and returning the samples more quickly at lower cost. This restructuring involves modifications to the mission architecture, including the simplification of the sample retrieval process and the potential downsizing of mission components.

As part of these adjustments, JPL, the primary institution responsible for MSR program development, has faced budgetary constraints leading to workforce reductions. In late 2023, JPL announced layoffs impacting several hundred employees, spanning various departments and projects. These layoffs are part of broader cost-cutting measures intended to ensure the long-term viability of the MSR program and other critical projects. While these changes have introduced challenges, JPL remains committed to its pioneering role in space exploration and the successful completion of Mars Sample Return.

JPL continues to push the boundaries of space exploration with ambitious future missions. Upcoming projects beyond MSR include the Europa Clipper, which aims to investigate the potential habitability of Jupiter's moon Europa, and a concept for a high-altitude helicopter on Mars, aiming to explore Martian surfaces inaccessible by rovers.

5 Low Energy Electron Diffraction/Auger Electron Spectroscopy

5.1 Background

Ices have been observed in various planetary environments, from ocean worlds and icy surfaces in the outer solar system to Kuiper Belt Objects (KBOs) and comets. The composition of these ices varies; they are mostly H_2O-dominated for icy surfaces of ocean worlds like Europa and Enceladus, and N_2-dominated beyond Neptune, [Brown, 2012, Roush, 2001]. The structural properties of these ices, such as crystallinity and grain size, reflect their formation history and impact their spectroscopic properties.

Currently, most planetary science studies on surface ices use infrared (IR) spectroscopy for structural determination. For example, much of the understanding of the state of ice on Europa and other bodies is derived from small shifts in position and band depth of a feature at 1.65 μm in IR spectra, [Berdis et al., 2022]. However, IR spectroscopy only probes the immediate environment of molecules, which depends on several factors including crystallinity, composition (e.g., presence of salts), and temperature. This can lead to ambiguities in data interpretation.

Diffraction techniques, on the other hand, probe interatomic spacings and provide clear and precise information about crystalline structures. Although JPL is equipped with an X-ray diffraction instrument that has provided significant insights into the crystalline structures of planetary-relevant ices, this instrument cannot operate at the low temperatures (< 77K) and low pressures that are relevant for most icy moons and KBOs, [Schmitt et al., 1989].

To overcome these limitations, the project aims to utilize Low Energy Electron Diffraction (LEED) and Auger Electron Spectroscopy (AES), techniques rarely applied in planetary science. LEED and AES are particularly suited for examining the crystalline structures of ices at the extremely low temperatures and pressures typical of outer solar system bodies.

5.2 Theory

5.2.1 LEED

Low-Energy Electron Diffraction (LEED) is a powerful surface science technique used to investigate the crystalline structure of materials. It is particularly useful for studying the topmost atomic layers of a crystal, which are often critical in determining the material's surface properties. LEED is widely used in surface physics, chemistry, and materials science to gain insights into surface reconstructions, defects, and adsorbate interactions, [Attard and Barnes, 2011]. This method is separated into three phenomena:

- **Electron Bombardment**: In LEED, a beam of low-energy electrons (typically in the range of 20-200 eV) is directed at the surface of the sample. The electrons interact with the surface atoms, causing them to scatter.

- **Diffraction**: The scattered electrons interfere with each other, producing a diffraction pattern that is characteristic of the arrangement of atoms on the surface. The diffraction pattern is influenced by the periodicity and symmetry of the surface atomic lattice.

$$n\lambda = 2d\sin(\theta) \tag{1}$$

where n is the order of diffraction, λ is the wavelength of the electrons, d is the spacing of the atomic planes, and θ is the diffraction angle. This equation describes the constructive interference condition for electron waves scattered by the atomic planes.

- **Detection**: The diffraction pattern is captured on a fluorescent screen or by using electronic detectors. By analyzing the positions and intensities of the diffraction spots, one can deduce the surface structure, including the lattice parameters and any surface reconstructions.

$$\lambda = \frac{h}{\sqrt{2meV}} \tag{2}$$

where h is Planck's constant ($6.626 \times 10^{-34}\,\mathrm{J{\cdot}s}$), m is the electron mass ($9.109 \times 10^{-31}\,\mathrm{kg}$), e is the electron charge ($1.602 \times 10^{-19}\,\mathrm{C}$), and V is the accelerating potential. This equation relates the wavelength of the electrons to their kinetic energy, which is crucial for interpreting LEED patterns, [Attard and Barnes, 2011].

This method is used to identify the arrangement of atoms on surfaces. It provides detailed information about the periodicity and symmetry of surface structures, which is essential for understanding surface phenomena, [Attard and Barnes, 2011]. Many materials undergo surface reconstructions, where the surface atomic arrangement differs from the bulk structure. LEED is a primary tool for studying these reconstructions, providing insights into how surfaces adapt to minimize energy. LEED can also be used to study molecules adsorbed on surfaces, revealing how they interact with and modify the surface structure. This is important for catalysis, sensor development, and other surface-related technologies.

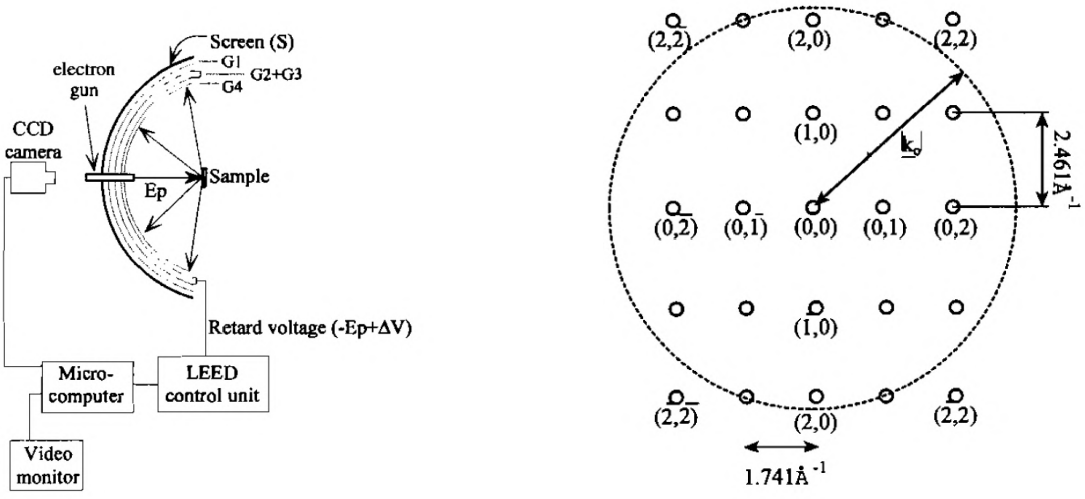

(a) LEED Instrument (b) Example of LEED pattern

Figure 3: LEED Instrument *S*ource: Attard and Barnes [2011]

5.2.2 AES

Auger Electron Spectroscopy (AES) is a highly sensitive surface analytical technique used to determine the elemental composition of surfaces. AES is based on the Auger process, a multi-electron phenomenon where the ejection of an electron leads to the emission of a second electron, known as the Auger electron, [Attard and Barnes, 2011]. AES is widely used in materials science, chemistry, and nanotechnology for its ability to provide detailed chemical information from the top few atomic layers of a material, [Attard and Barnes, 2011]. This method is separated into three phenomena:

- **Excitation**: In AES, a high-energy electron beam (typically 2-10 keV) is directed at the sample surface, causing the ejection of a core electron from the atom. This creates a core-level vacancy, [Attard and Barnes, 2011].

- **Relaxation**: The atom relaxes by having an electron from a higher energy level fall into the vacancy. The energy released in this process is transferred to another electron, which is then ejected from the atom as an Auger electron.

$$E_K = E_i - E_j - E_k \tag{3}$$

  where E_K is the kinetic energy of the Auger electron, E_i is the binding energy of the initial vacancy, E_j and E_k are the energies of the electrons filling the vacancy and being ejected, respectively. This equation describes the energy balance involved in the Auger process and is fundamental to interpreting AES spectra, [Attard and Barnes, 2011].

- **Detection**: The ejected Auger electrons are detected and their kinetic energy is measured. The kinetic energy of the Auger electrons is characteristic of the element from which they were emitted, allowing for the identification of the surface composition, [Attard and Barnes, 2011].

The Auger spectrum is a plot of the intensity of detected electrons as a function of their kinetic energy and is the final result of this study. Each chemical element produces characteristic peaks in the spectrum, corresponding to specific Auger transitions of that element. By analyzing these peaks, one can determine the presence and concentration of elements on the surface. Auger electrons therefore allow us to determine the composition of a material or the arrangement of an alloy, or the progress of a chemical reaction (oxidation, etc.).

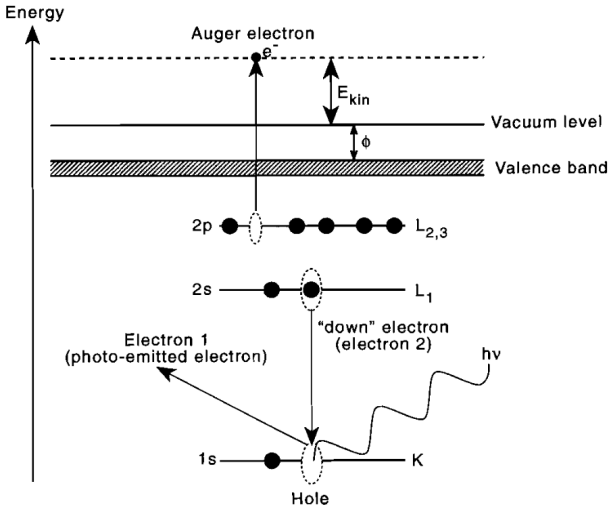

Figure 4: AES Theory *S*ource: Attard and Barnes [2011]

LEED and AES are complementary techniques for surface analysis. LEED provides detailed information about the crystalline structure of surfaces, making it indispensable for studying surface reconstructions and atomic arrangements. AES, on the other hand, offers precise chemical composition analysis, allowing researchers to identify and quantify elements on the surface and investigate their chemical states, [Attard and Barnes, 2011]. Together, these techniques offer a comprehensive toolkit for studying material surfaces, essential for advancements in materials science, surface chemistry, and nanotechnology, [Attard and Barnes, 2011].

5.3 Instrument assembly

The project involves adapting an existing LEED instrument to an extreme-high vacuum system ($< 10^{-10}$Torr) where ice samples can be grown on a cryogenic substrate at temperatures above 8K. The ultra-high vacuum system is composed of three pumps (from Agilent): a dry scroll pump, a turbo pump, and an ion pump, all working together to achieve a pressure of approximately 10^{-9}Torr in the chamber. The system also includes a cryostat for sample deposition, which is currently not mounted and is temporarily replaced by a non-cryogenic arm.

Additionally, the setup features multiple valves to ensure proper compartmentalization of the instrument, three pressure sensors each covering different pressure ranges, and two specially treated windows to potentially add an infrared dimension to the system. The LEED/AES instrument used in this setup is the BDL800IR model from OCIVM. The entire system is monitored and controlled by several acquisition/control units.

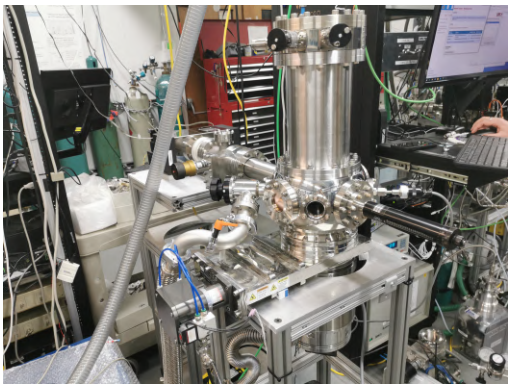

(a) Vacuum Chamber

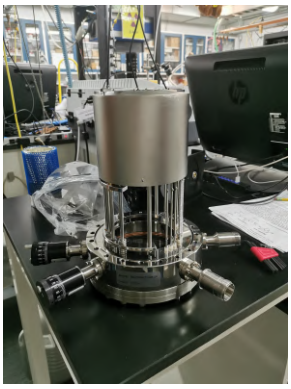

(b) LEED

Figure 5: Assembly

Unfortunately, during the initial startup, the system detected a degradation in the Wehnelt electrode inside the electron gun of the LEED, which has halted the project. The instrument is currently awaiting funding or a decision on repair or replacement.

5.4 Perspective of evolution

Despite the current setback due to the damaged Wehnelt electrode, there are several future perspectives for the project. One primary objective is to repair the instrument and conduct initial tests of the AES on a silicon sample. Following this, the cryostat will be installed to enable temperature-controlled experiments.

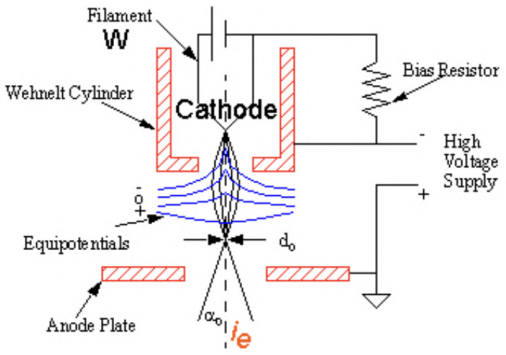

Figure 6: Electron Gun *S*ource: Liao [2006]

Once operational, the project aims to utilize LEED to observe the surface of ice under low pressure and low temperature conditions, specifically focusing on the transition from the amorphous to the crystalline phase of CO_2. By addressing the shortcomings of current techniques, this project will enhance our understanding of ice crystallinity in planetary environments, providing more accurate data for interpreting spectroscopic observations and contributing significantly to the advancement of planetary science.

6 Comet project

The project, led by Dr. Bjorn Davidsson, a researcher from the Planetary Science section at JPL, focuses on developing simulation models, particularly concerning comets. The role of the laboratory group within the Planetary Science section in this project is to provide experimental data to support these models. The primary objective is to gain a deeper understanding of cometary processes and to compare the results with data from ESA's Rosetta Philae mission.

In this context, my role has been to study the sublimation of CO during the crystallization of CO_2. This involves conducting experiments to observe and analyze the behavior of these gases under controlled conditions, contributing valuable data that can be used to validate and refine the simulation models developed by Dr. Bjorn Davidsson and his team.

6.1 Background

The European Space Agency's Rosetta mission, specifically its Philae lander, made groundbreaking discoveries during its study of comet 67P/Churyumov-Gerasimenko. One of the significant findings was the detection of numerous molecules, including carbon monoxide (CO), trapped within an amorphous phase of carbon dioxide (CO_2), [Bockelee-Morvan et al., 2004].

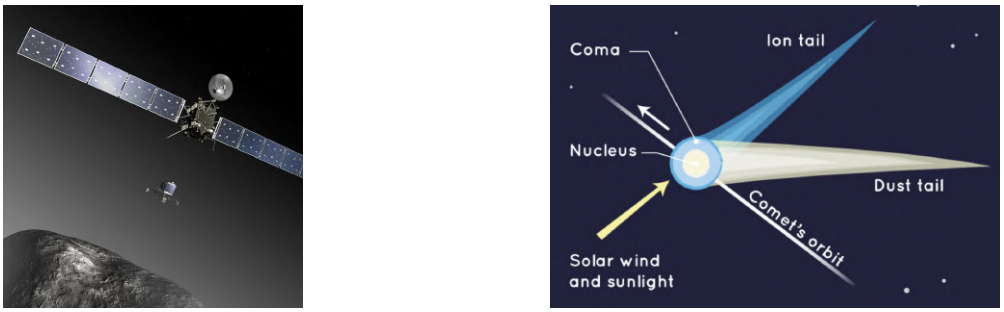

(a) Rosetta Philae mission (b) Comet schematic

Figure 7: Rosetta Philae *S*ources: Wikipedia [b], Spaceplace

In the context of cometary science, understanding the transition between amorphous and crystalline phases of CO_2 and their interactions with trapped volatiles such as CO is essential.

Amorphous CO_2 is a non-crystalline solid where the molecules are arranged randomly. This phase is typically formed under rapid cooling conditions, such as those found in the outer regions of the solar system where temperatures can plummet rapidly. Amorphous solids have higher internal energy compared to their crystalline counterparts and can trap other molecules, such as CO, within their disordered structure. This trapping occurs because the rapid cooling does not allow the molecules enough time to organize into a crystalline lattice, [Smith, 2011].

When amorphous CO_2 undergoes thermal processing, it can transition to a crystalline phase. Crystalline CO_2 has a well-ordered molecular structure and is more thermodynamically stable. This phase transition releases the trapped molecules due to the rearrangement of the CO_2 molecules into a more stable lattice, [Smith, 2011].

The sublimation rate of CO from the amorphous CO_2 matrix can be described by the following Arrhenius-type equation:

$$R(T) = A \exp\left(-\frac{E_a}{RT}\right)$$

where $R(T)$ is the sublimation rate, A is the pre-exponential factor, E_a is the activation energy, R is the gas constant, and T is the temperature, [hage et al., 1993].

Including the sublimation dynamics of CO from amorphous CO_2 in cometary models improves the accuracy of predictions regarding the composition and behavior of the comet's coma and tail. The release of CO influences the mass loss rates, jet formations, and the overall activity of the comet, [Bockelee-Morvan et al., 2004].

Understanding the crystallization kinetics of CO_2 and the associated sublimation of CO provides insights into the thermal history of the comet. It helps in determining the past environmental conditions the comet has experienced and the processes it has undergone, [Bockelee-Morvan et al., 2004].

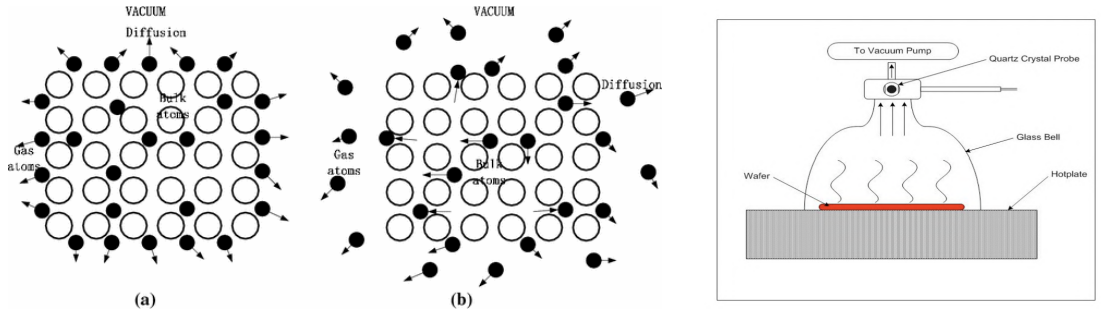

(a) Sublimation process (b) Instrument visualisation

Figure 8: Experiment process *S*ources: Luo et al. [2016], Carr et al. [2006]

The study of CO sublimation during the crystallization of CO_2 in comets, as observed by the Rosetta mission, is a crucial aspect of understanding cometary behavior and evolution. By quantifying the sublimation rates and integrating this information into models, researchers can better predict the activity and physical characteristics of comets. This knowledge not only enhances our understanding of these ancient celestial bodies but also provides insights into the early solar system's conditions and the processes that shaped it, [Bockelee-Morvan et al., 2004].

6.2 KOALA Intrument

The KOALA setup consists of an ultra-high vacuum (UHV) chamber, equipped with three pumps to achieve and maintain the required vacuum conditions. These pumps include a dry scroll pump, a turbo pump, and an ion pump, working together to achieve

a pressure of approximately 10^{-10} Torr in the chamber. This ultra-high vacuum environment is essential for accurate measurements of sublimation processes and to prevent contamination from residual gases.

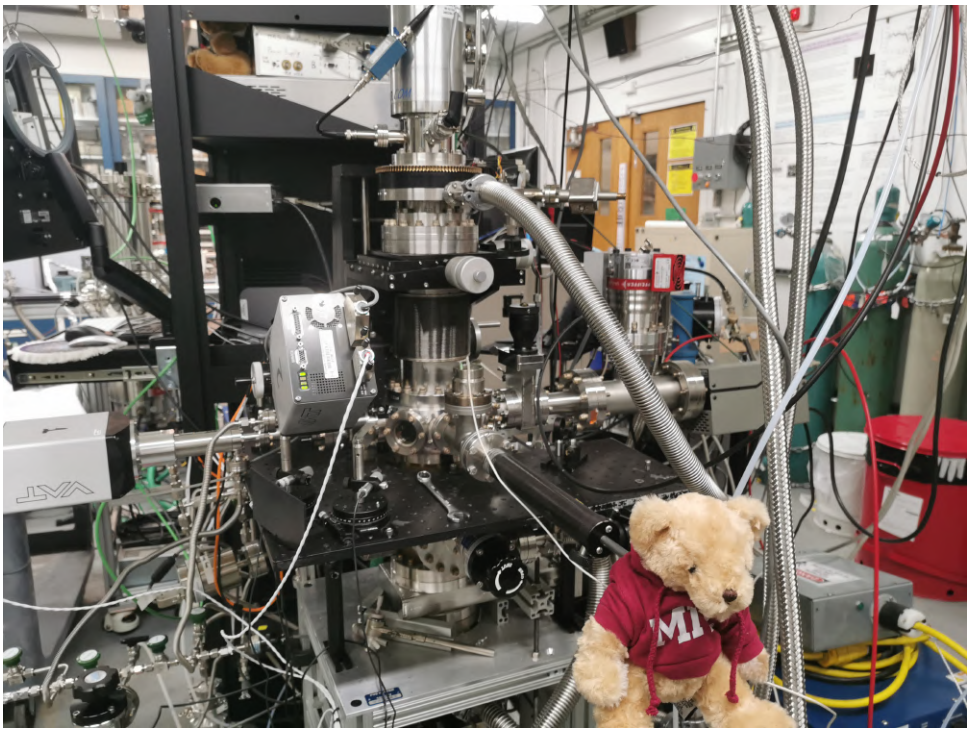

Figure 9: KOALA Instrument

One of the critical components of the KOALA setup is the quartz crystal microbalance (QCM). The QCM is equipped with a polycrystalline gold layer on a quartz wafer, which is used to measure the mass changes of the sample with high precision. This allows us to monitor the sublimation rate of CO in real-time as the mass of the sublimated molecules is detected as a change in the oscillation frequency of the quartz crystal. In addition to the QCM, the KOALA setup includes a quadrupole mass spectrometer (QMS). The QMS is used to analyze the residual vacuum conditions and to detect desorbed species during the sublimation process. This provides valuable information on the composition of the gases released from the ice and helps to identify any contaminants or unexpected desorption products.

6.2.1 Theory

The Quartz Crystal Microbalance (QCM) is a highly sensitive mass measurement device that operates based on the piezoelectric properties of quartz crystals. The fundamental principle of the QCM is that a change in mass on the surface of the quartz crystal results in a change in its resonance frequency. This relationship is quantitatively described by the Sauerbrey equation, which allows for precise determination of the mass changes.

A quartz crystal is an oscillating device that operates at a specific resonance frequency. When an alternating electric field is applied to the crystal, it induces mechanical vibrations due to the piezoelectric effect. The resonance frequency f of the crystal is given

by:

$$f = \frac{1}{2d}\sqrt{\frac{\mu}{\rho}}$$

where d is the thickness of the quartz crystal, μ is the shear modulus of quartz, and ρ is the density of quartz, Songkhla and Nakamoto [2021]. These parameters are critical in defining the fundamental frequency at which the quartz crystal oscillates. Any additional mass on the crystal surface will alter this frequency, which brings us to the application of the Sauerbrey equation.

The Sauerbrey equation establishes a linear relationship between the change in the resonance frequency Δf and the change in mass Δm per unit area on the surface of the quartz crystal. This equation is valid under the assumption that the added mass is rigidly coupled to the crystal surface and the added mass is small compared to the mass of the crystal. The Sauerbrey equation is expressed as:

$$\Delta f = -\frac{2f_0^2 \Delta m}{A\sqrt{\mu\rho}}$$

where Δf is the change in frequency, f_0 is the fundamental resonance frequency of the crystal, Δm is the mass change per unit area, A is the active area of the crystal, μ is the shear modulus of quartz, and ρ is the density of quartz, Sauerbrey [1959], Songkhla and Nakamoto [2021]. This relationship allows us to precisely measure the mass changes on the quartz crystal surface by monitoring the frequency shifts.

By rearranging the Sauerbrey equation, we can solve for the mass change Δm:

$$\Delta m = -\frac{A\sqrt{\mu\rho}}{2f_0^2}\Delta f$$

The negative sign indicates that an increase in mass results in a decrease in frequency, which is a direct consequence of the piezoelectric effect.

In the KOALA setup, the QCM is used to monitor the sublimation of CO from the CO_2 matrix. As CO molecules sublimate and leave the surface of the quartz crystal, the resulting decrease in mass leads to an increase in the resonance frequency. By continuously measuring the frequency changes, we can determine the rate of sublimation and the total mass of CO that has sublimated over time.

6.2.2 Experiment

In this experiment, the CO and $^{13}CO_2$ gases were directly mixed in the ultra-high vacuum chamber, with the ratio being controlled by the Quadrupole Mass Spectrometer (QMS) to ensure a 3:1 ratio of ice. The deposition temperature was set to 14K. Subsequently, we conducted the experiment at various temperatures ranging from 57.5K to 65K. The use of $^{13}CO_2$, as opposed to regular $^{12}CO_2$, was to enable the QMS to better differentiate its presence.

The primary objective of this experiment was to determine the outgassing kinetics and the mass of sublimated CO. This data is crucial for the simulation team, as it allows

them to accurately determine the sublimation rate as a function of temperature. By understanding the sublimation kinetics, we can improve the models that predict the behavior of cometary ices under various thermal conditions.

6.2.3 Result

The first graph (Figure 10) shows the mass of CO sublimated over a period of 4 hours at various temperatures, determined using the Sauerbrey equation. We observed that at 65K, the data points showed higher values. The graph also indicates that an increase in temperature does not necessarily result in an increase in sublimation. Additionally, the overshoot due to the temperature increase is clearly visible. Additionally, this graph highlights the reproducibility issues encountered. Specifically, the curve at 62.5K, which was repeated twice, showed discrepancies.

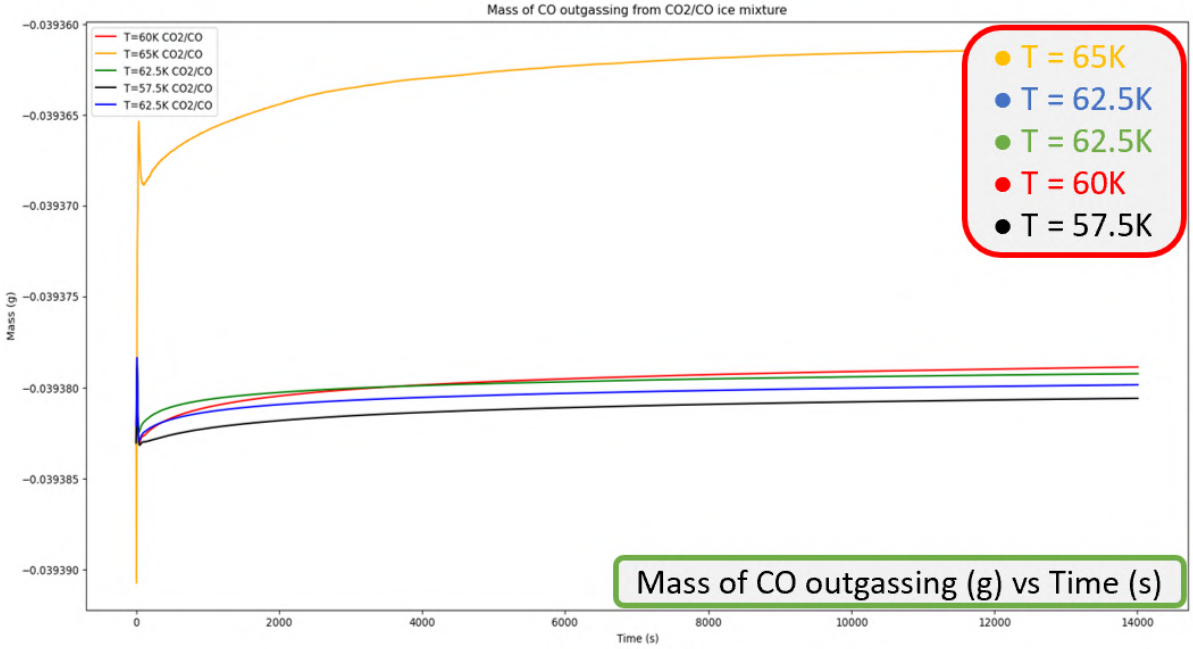

Figure 10: Mass of CO Sublimated Over 4 Hours at Various Temperatures

The second graph (Figure 11) presents the mass derivation observed by the microbalance, along with the CO and $^{13}CO_2$ signals from the QMS, over a temperature ramp of 1K/min (Temperature Program desorption). It shows that CO begins to sublimate around 40K, while $^{13}CO_2$ starts to sublimate at approximately 80K. This reassures us that the microbalance is indeed observing CO sublimation and not $^{13}CO_2$.

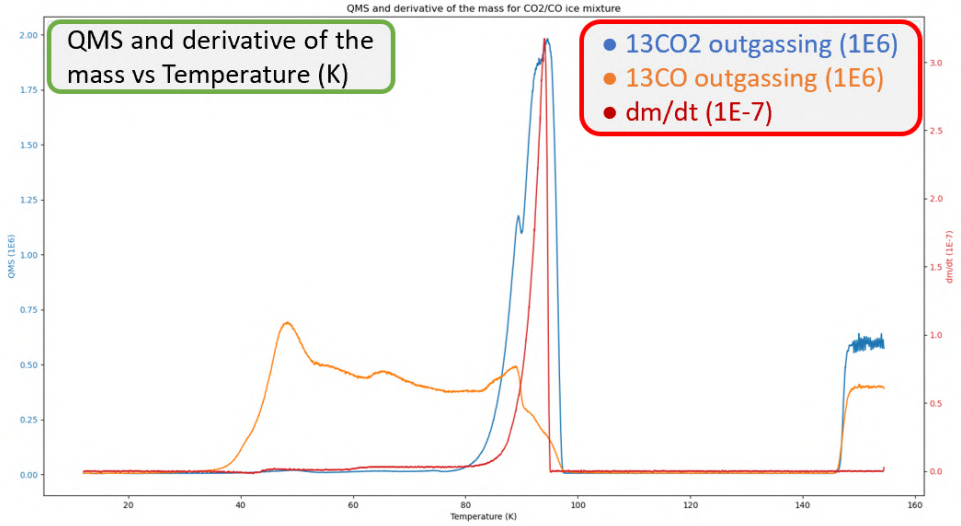

Figure 11: Mass Derivation by Microbalance with QMS Analysis of CO and $^{13}CO_2$ During a Temperature Ramp

However, this graph raises an issue as the mass derivation should be a multiple of the CO curve observed by the QMS, according to the Sauerbrey equation. This discrepancy suggests potential problems with the deposition process. We suspect that during deposition, directed by the QMS, some of the sample may be lost in the chamber rather than being deposited on the microbalance. This leads us to believe that the QMS is detecting elements that are not being deposited on the microbalance. Additionally, the study of the TPD (Temperature Programmed Desorption) reveals that within our temperature range, an increase in temperature does not necessarily result in a corresponding increase in the sublimation rate of CO. This indicates that there are other factors at play that must be considered to accurately quantify sublimation.

The results obtained from the KOALA instrument indicate several critical issues. The mass derivation discrepancy, when compared to the QMS data, highlights possible deposition inefficiencies. Finally, the uncertainty in the deposition ratio, aimed to be 3:1, and reproducibility issues mean that alternative experimental methods may be more appropriate for this project. To check these values we use the LEFTY setup.

6.3 LEFTY Intrument

The instrument in the laboratory, named LEFTY, consists of the following components: an ultra-high vacuum (UHV) chamber, an Ar transparent window, a vapor inlet, a Bruker Vertex 80v FTIR infrared spectrometer under vacuum covering a range of 4000 to 600 cm^{-1} (mid-infrared), a closed-cycle helium cryostat, two silicon diodes and a resistor for temperature measurement.

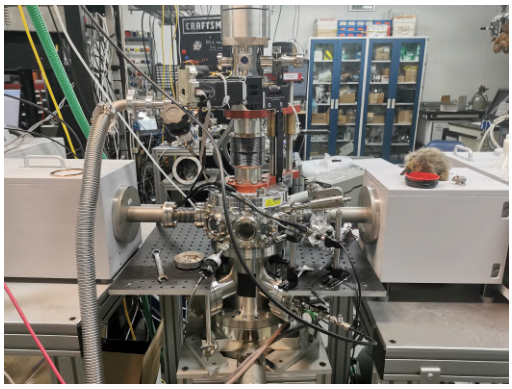

Figure 12: LEFTY Setup

6.3.1 Theory

Fourier Transform Infrared (FTIR) Spectroscopy is a sophisticated analytical technique widely used to identify chemical compounds and investigate molecular structures by examining the infrared (IR) absorption spectra. The principle of FTIR relies on the fact that molecular vibrations occur at specific frequencies, which correspond to distinct IR wavelengths. When a molecule absorbs IR radiation, the absorbed wavelengths cause vibrations within the molecule, which are characteristic of its specific structure.

FTIR spectroscopy involves the interaction of infrared radiation with matter, measuring the wavelengths and intensities of the absorption of IR radiation by a sample. The technique is based on several key components and processes:

- The core of FTIR spectroscopy is the Michelson interferometer. It consists of a beam splitter, a fixed mirror, and a moving mirror. The beam splitter divides the incoming IR beam into two paths: one reflected to the fixed mirror and the other transmitted to the moving mirror. These beams are then recombined, creating an interference pattern that changes as the moving mirror shifts position, [Griffiths and de Haseth, 2007].

- The recombined beams produce an interferogram, a signal that contains all the infrared spectral information of the sample. The interferogram represents the intensity of the IR signal as a function of the optical path difference caused by the moving mirror, [Griffiths and de Haseth, 2007].

- The interferogram is subjected to a mathematical process called Fourier transform, which converts the time-domain data into a frequency-domain spectrum. The resulting IR spectrum displays absorbance (or transmittance) as a function of wavenumber (inverse of wavelength, typically in cm^{-1}), [Griffiths and de Haseth, 2007]. The Fourier transform is mathematically defined as:

$$F(\nu) = \int_{-\infty}^{\infty} f(t) \cdot e^{-2\pi i \nu t} \, dt$$

Molecules exhibit specific vibrational modes, such as stretching, bending, and twisting, which occur at characteristic frequencies. These modes create a unique spectral fingerprint for each molecule, allowing for precise identification, [Griffiths and de Haseth, 2007].

The IR spectrum provides detailed information about the molecular structure through these vibrational signatures.

- Stretching Vibrations: These occur when the distance between two atoms increases or decreases along the bond axis. Stretching can be symmetric or asymmetric.
- Bending Vibrations: These involve changes in the angle between two bonds. Bending vibrations include scissoring, rocking, wagging, and twisting motions, [Griffiths and de Haseth, 2007].

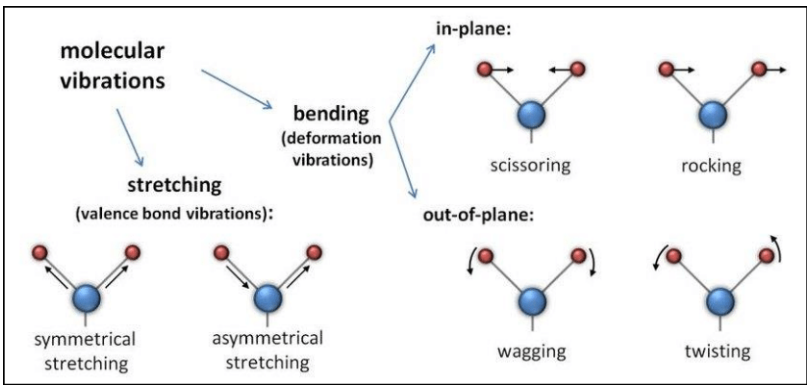

Figure 13: Vibrational Signatures *S*ource: Mutsaers [2018]

FTIR spectroscopy is invaluable in the study of space, particularly in the analysis of extraterrestrial materials and atmospheres. The technique provides insights into the composition and molecular structure of cosmic dust, meteorites, comets, planetary atmospheres, and interstellar clouds, [Bockelee-Morvan et al., 2004].

Comets contain primordial material from the early solar system. By analyzing the infrared spectra of comets, scientists can determine the composition of their nuclei and coma, shedding light on the solar system's formation and evolution. The Rosetta mission, which studied comet 67P/Churyumov-Gerasimenko, utilized infrared spectroscopy to identify water ice, carbon dioxide, and organic compounds on the comet's surface, [Watanabe and Kouchi, 2008].

The interpretation of FTIR spectra relies on understanding the interaction between infrared radiation and molecular vibrations. The fundamental equation governing this interaction is derived from the Beer-Lambert Law, which relates the absorbance (A) to the concentration (c) of the absorbing species, path length (b), and molar absorptivity (ϵ):

$$A = \epsilon \cdot b \cdot c$$

FTIR spectroscopy is a critical tool in space research, providing detailed molecular information that helps scientists understand the composition and processes of extraterrestrial environments. By analyzing the IR spectra of planetary atmospheres, comets, interstellar media, and meteorites, researchers gain valuable insights into the formation and evolution of the solar system and the universe, [Bockelee-Morvan et al., 2004, Watanabe and Kouchi, 2008].

6.3.2 Experiment

To begin, we conducted experiments on well-documented compounds in scientific literature. These experiments on H_2O aimed to familiarize ourselves with the instrumentation and validate our methodology.

Firstly, we observed the crystallization of water under varying temperature ranges between 130 K and 140 K. The objective was to monitor the spectral shift associated with the transition from amorphous to crystalline state. This transition is well-documented, allowing us to compare our results with existing literature. Similarly, we studied the crystallization of pure $^{12}CO_2$ at temperatures ranging from 50 K to 62 K. As with water, the goal was to observe the spectral shift during the transition from amorphous to crystalline $^{12}CO_2$, and to validate our experimental setup against known data.

After validating our methodology with water and pure $^{12}CO_2$, we moved on to a more complex study focusing on the sublimation of carbon monoxide (CO) in a transition of amorphous to crystallize $^{13}CO_2$ phase. This study required a preliminary preparation of the gas mixture.

The mixture of $^{13}CO_2$ and CO was prepared in a glass balloon, with a ratio of 3:1 (three units of $^{13}CO_2$ to one unit of CO). This step was crucial to ensure the homogeneity of the mixture before forming the amorphous phase. The experiments were conducted under precisely controlled temperatures to observe sublimation and crystallization phenomena.

The primary objectives were to study the sublimation kinetics of CO from the amorphous $^{13}CO_2$ matrix and to investigate the impact of CO presence on $^{13}CO_2$ crystallization. By analyzing the shifts observed in the FTIR spectra, we gained insights into the interactions between these molecules during the phase transition process.

6.3.3 Result

H_20 We began our study by analyzing the FTIR spectrum of water (H_2O). Our goal was to observe the spectral shifts that occur during the transition from amorphous to crystalline states. Below is the FTIR spectrum of water (Figure 14), a table that allows the identification of the mode of vibration based on the position of the peak (Figure 15), along withn a view highlighting the shifts during crystallization (Figure 16).

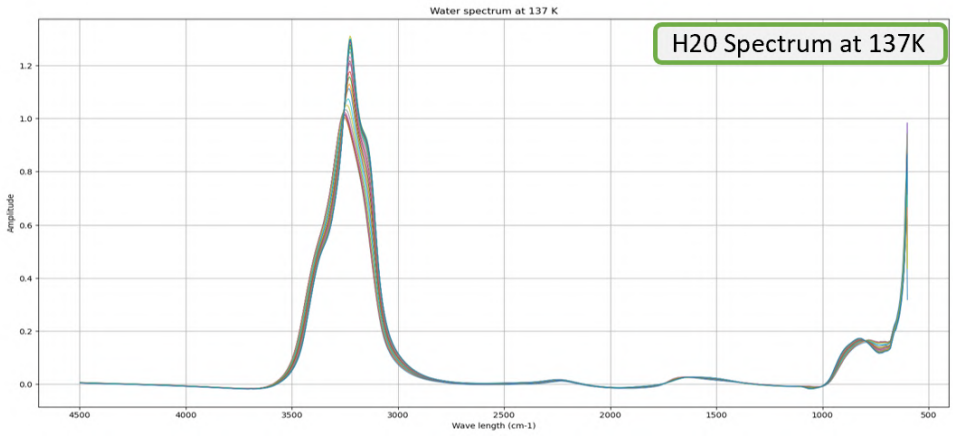

Figure 14: H_2O FTIR spectrum

Ice	Mode	Band Position cm^{-1} (μm)	A_{14K} cm molec^{-1}	A_{60K}/A_{14K}	A_{60K} cm molec^{-1}	A_{100K}/A_{14K}	A_{100K} cm molec^{-1}
H_2O	O–H stretch	3280 (3.045)	2.0(-16)[a]				
	O–H bend	1660 (6.024)	1.2(-17)				
	libration	760 (13.16)	3.1(-17)				
CO.....	^{12}C≡O stretch	2139 (4.675)	1.1(-17)[b]				
	^{13}C≡O stretch	2092 (4.780)	1.3(-17)				
CO_2	(ν_3) ^{12}C=O stretch	2343 (4.268)	7.6(-17)[c]	0.98	7.4(-17)	0.97	7.4(-17)
	(ν_3) ^{13}C=O stretch	2283 (4.380)	7.8(-17)	0.94	7.3(-17)	0.92	7.2(-17)
	(ν_2) O=C=O bend	660,665 (15.15,15.27)	1.1(-17)	1.03	1.1(-17)	1.04	1.1(-17)
	($\nu_1 + \nu_3$) combination	3708 (2.697)	1.4(-18)	1.05	1.5(-18)	1.08	1.5(-18)
	($2\nu_2 + \nu_3$) combination	3600 (2.778)	4.5(-19)	1.22	5.5(-19)	1.20	5.4(-19)

Figure 15: Vibration wavelength *S*ource: Gerakines et al. [1994]

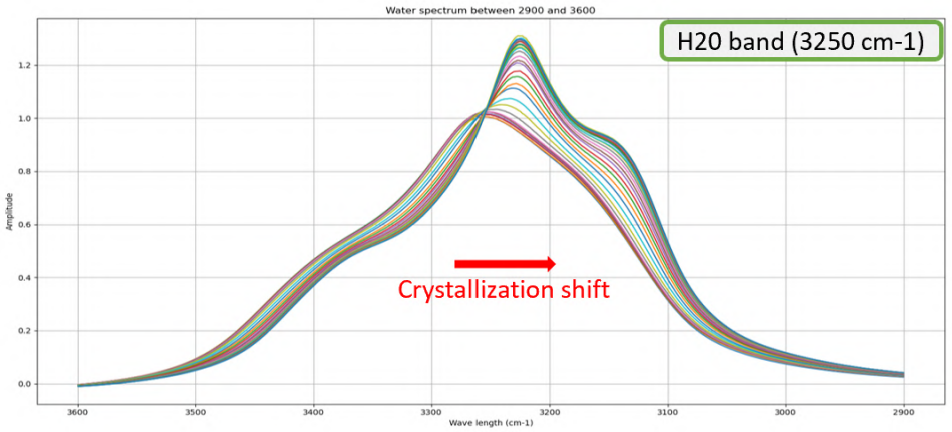

Figure 16: H_2O shift

To quantify the crystallization process, we performed a Pearson correlation analysis between the spectra of amorphous, crystalline, and intermediate states of water. This correlation quantitatively measures the degree of similarity between spectral data sets. During crystallization, changes in the molecular structure of a material are reflected as shifts or variations in the FTIR spectrum. By applying the correlation we can assess

the relationship between the spectra of the amorphous and crystalline phases, effectively tracking the progress of crystallization. The Pearson correlation coefficient r is given by:

$$r = \frac{\sum_{i=1}^{n}(x_i - \bar{x})(y_i - \bar{y})}{\sqrt{\sum_{i=1}^{n}(x_i - \bar{x})^2 \sum_{i=1}^{n}(y_i - \bar{y})^2}}$$

where x_i and y_i are the spectral intensities at a given wavelength for the amorphous and crystalline states, respectively, and $\bar{x}$ and $\bar{y}$ are the mean intensities, [Howell, 2010].

By computing the Pearson correlation between the amorphous, crystalline, and intermediate spectra, we were able to track the degree of crystallization over time. Below is a graph showing the correlation coefficient as a function of time (Figure 17).

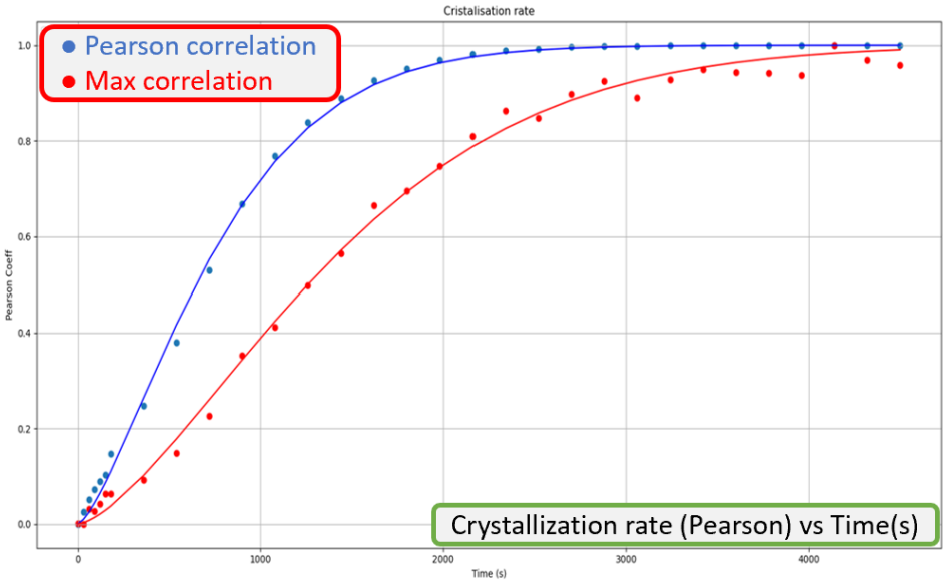

Figure 17: Crystallization evolution

In addition to Pearson correlation, we also compared the results with a simple linear correlation based on the maximum band strength of H_2O at 3200 cm^{-1}. The comparison revealed that both methods yield a JMAK curve for the degree of crystallization over time. The Johnson-Mehl-Avrami-Kolmogorov (JMAK) equation is described by:

$$X(t) = 1 - \exp\left(-Kt^n\right)$$

where $X(t)$ is the fraction of crystallized material at time t, K is the rate constant, and n is the Avrami exponent, [hage et al., 1993, Rath, 1995].

The JMAK model is well-suited for describing crystallization processes, where the transformation progresses through nucleation and growth mechanisms. This model is widely applied in materials science to describe phase transformations, including crystallization, [hage et al., 1993, Rath, 1995, Avrami, 1940].
We determined the crystallization time for various temperatures and compared our results with data from [Schmitt et al., 1989]. The crystallization time was plotted on a logarithmic scale against the temperature (Figure 18).

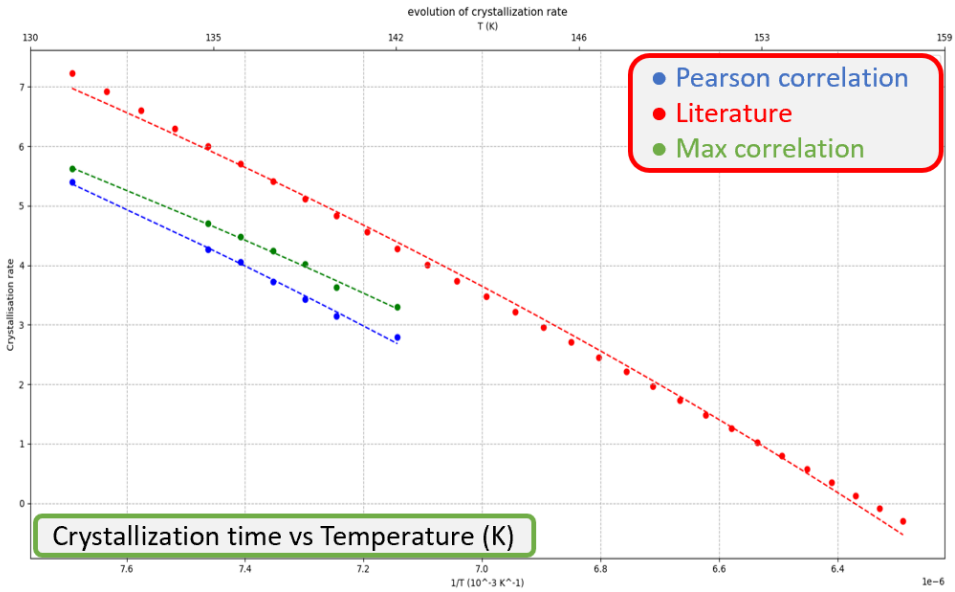

Figure 18: Crystallization rate

The slope of our experimental data was found to be similar to that reported in the literature, indicating that the Pearson correlation method is a reliable approach for determining crystallization time. The primary differences between our results and the published data can be attributed to variations in experimental setup, including differences in deposition and heating methods.

Using Pearson correlation to track the crystallization process provides a robust method for quantifying the degree of crystallization. Comparing our results with published data demonstrates the validity of our approach, despite minor differences due to experimental conditions.

Pure $^{12}CO_2$ Next, we studied the FTIR spectrum of pure $^{12}CO_2$. The FTIR spectrum (Figure 19 and 20) and the crystallization rate as a function of time (Figure 21) and temperature (Figure 22) are shown below.

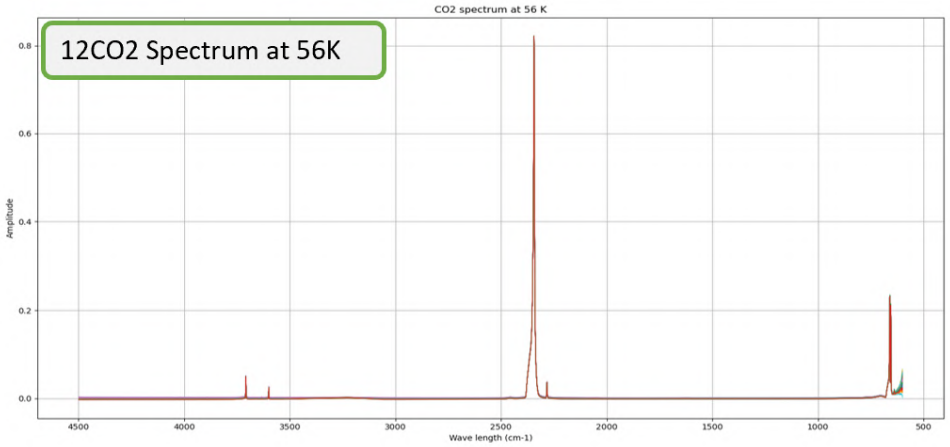

Figure 19: FTIR Spectrum of Pure $^{12}CO_2$

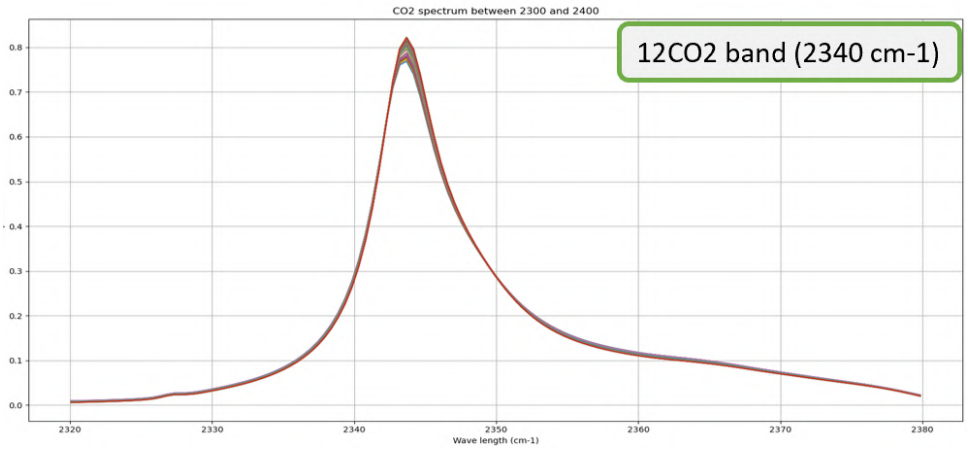

Figure 20: $^{12}CO_2$ Shift

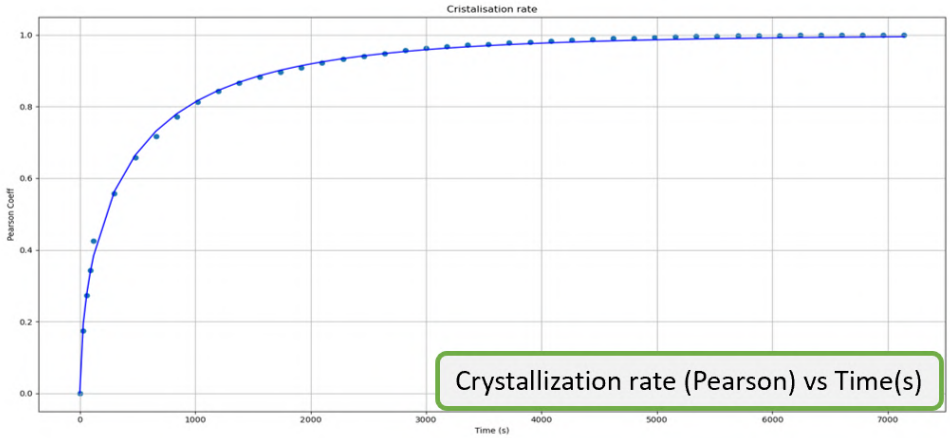

Figure 21: Crystallization Rate of $^{12}CO_2$ as a Function of Time

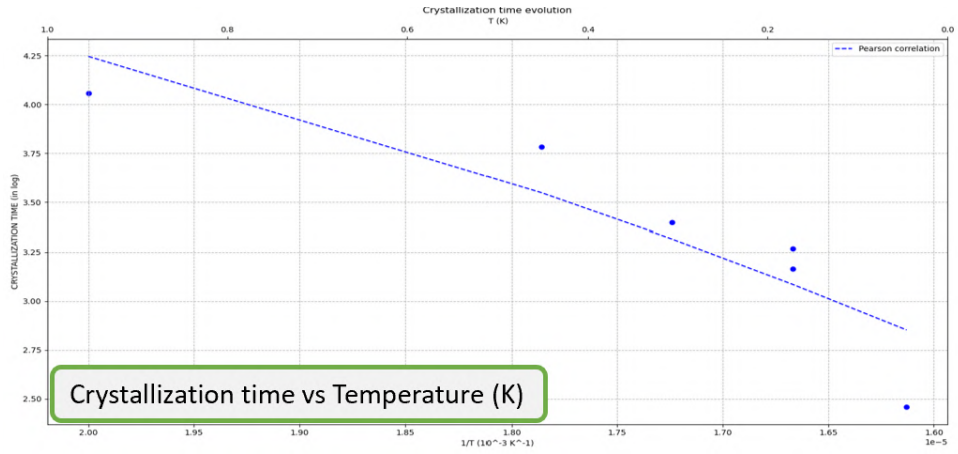

Figure 22: Crystallization Rate of $^{12}CO_2$ as a Function of Temperature

Finally, the crystallization of $^{12}CO_2$ was not visually clear, posing a challenge for the application of mathematical tools. Unlike water, we did not have a reference paper for comparison, and the observed shift was in the order of 2 to 3 points in the spectrum.

Consequently, it was difficult to ascertain whether crystallization had occurred or not. However, we do know that something is happening, as indicated by the evolution of the crystallization rate on the graph, which follows an exponential trend often associated with crystallization profiles. To confirm that crystallization is indeed occurring, it is necessary to employ additional study methods (such as Low-Energy Electron Diffraction).

CO-$^{13}CO_2$ mixture In the study of CO/$^{13}CO_2$, we focused on the CO band at 2140 cm^{-1}. By integrating the area under the curve, we related this area to the column density of molecules. The column density N in cm^{-2} is given by:

$$N = \int \frac{\tau}{A}\, dv$$

where τ is the optical depth and A is the absorption cross-section, [McQuarrie and Simon, 1997, Mangum and Shirley, 2015]. The optical depth τ is related to the absorbance A by:

$$\tau = \ln(10) \cdot A$$

We compared the integrated areas at various temperatures to study the sublimation kinetics of CO.
We also observed the shift in the $^{13}CO_2$ band during its crystallization to track the crystallization process. The results showed that as the temperature increased, more CO sublimated, as indicated by the decrease in the CO band area. However, the kinetics showed that lower temperatures resulted in faster sublimation kinetics, which contradicts our initial assumption.
Below are the graphs showing the FTIR spectrum (Figure 23), the CO band (Figure 24), the column density (Figure 25), and the spectral shifts (Figure 26). I also added the evolution of the $^{13}CO_2$/CO ratio (Figure 27). We can observe that the proportion of $^{13}CO_2$ within the mixture increases over time, which is logical since CO is sublimating from the ice. To assess the reliability of this observation, I included error bars on the graph, assuming a spectrum noise error of approximately 0.004 in amplitude. The data indicates that the initial ratio is around 2.41, rather than 3 as previously mentioned.

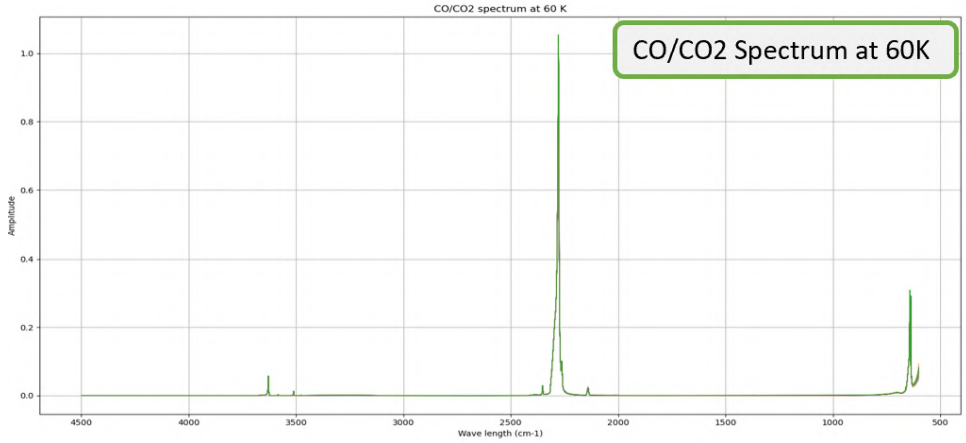

Figure 23: FTIR Spectrum of the CO/$^{13}CO_2$ Mixture

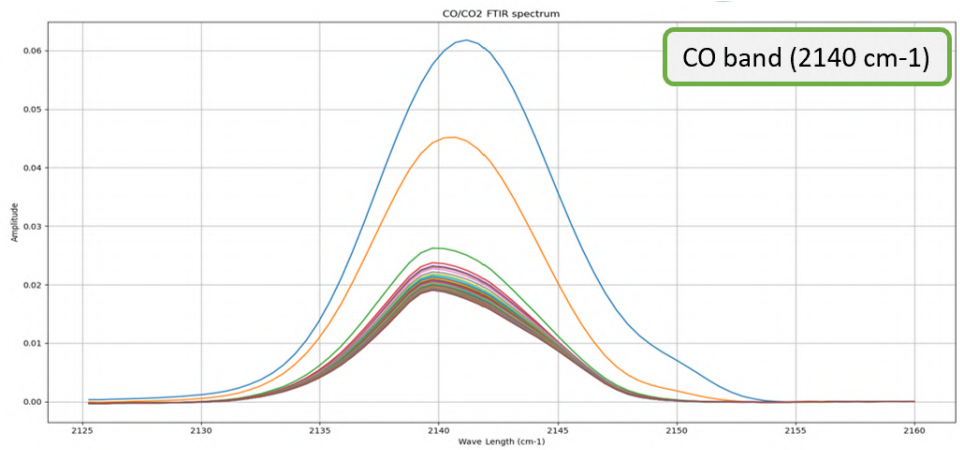

Figure 24: FTIR Spectrum of the CO Band

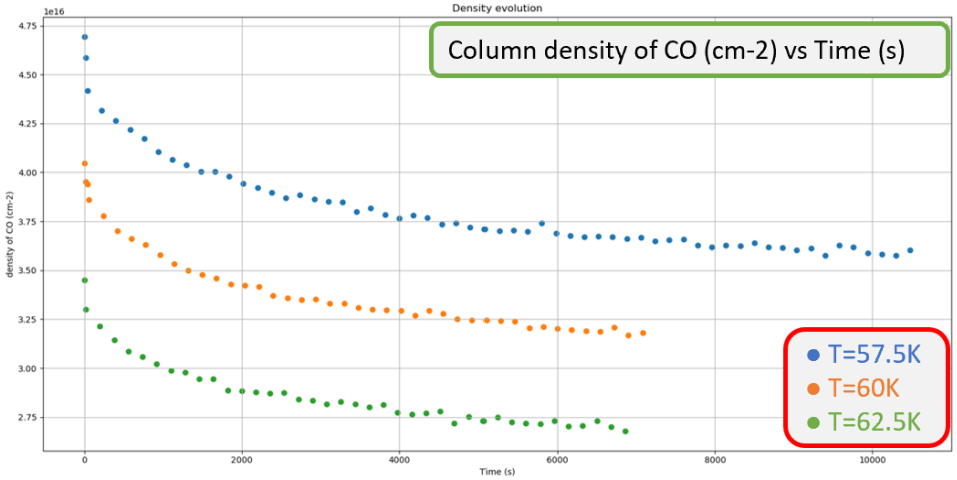

Figure 25: Column Density

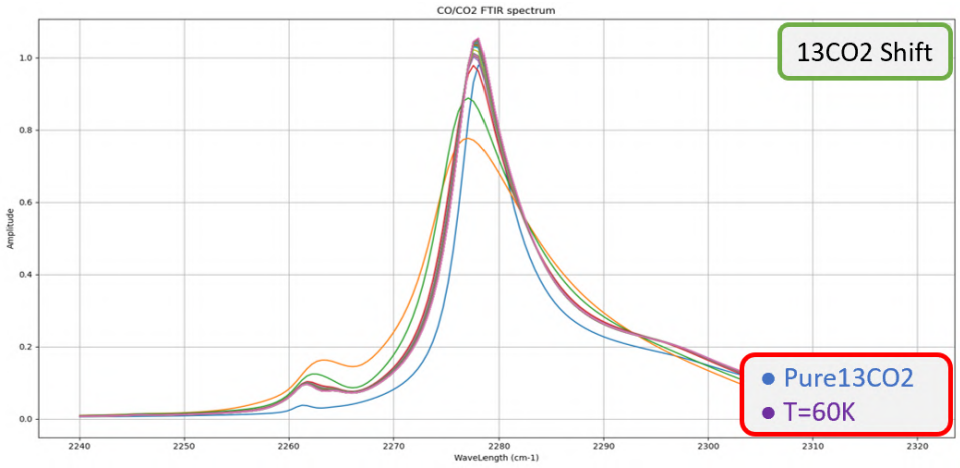

Figure 26: Spectral Shift of $^{13}CO_2$

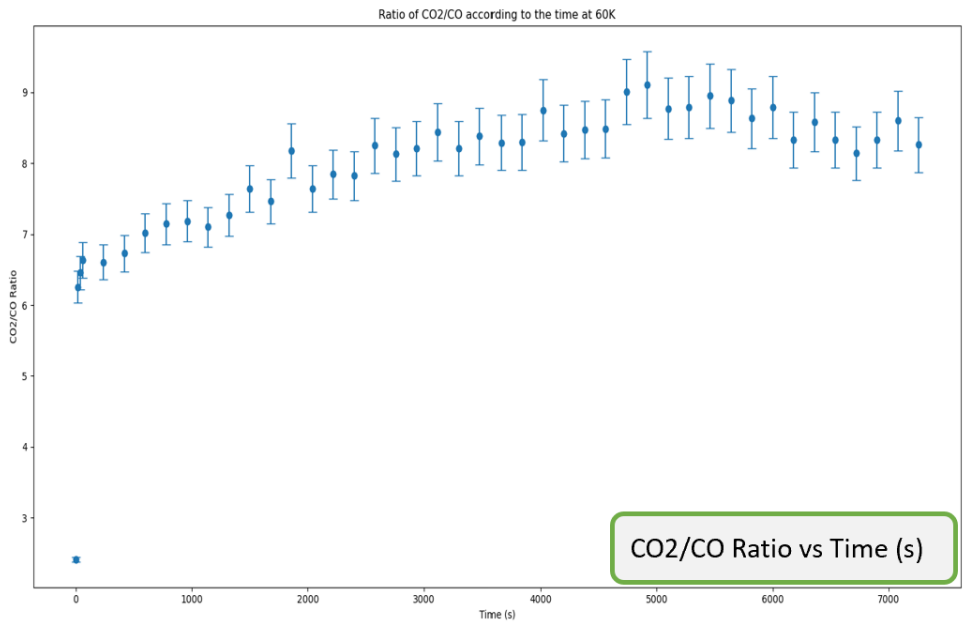

Figure 27: $^{13}CO_2/CO$ ratio

This FTIR spectroscopy study provided indispensable real sublimation data for simulation models. However, there remains uncertainty regarding the confirmed relationship between temperature and sublimation rate (As shown in the TPD study). Future projects could be supplemented by using LEED to ensure the crystallization of $^{13}CO_2$ or by employing an effective QMS to link observations from the spectroscopy to the number of sublimated molecules. The major question is regarding the deposition method. For this deposition, we use a pipette oriented towards the window holding the sample in front of the spectrometer and control the deposition using a photodiode and a laser to determine the thickness of the film studied. Thus, we may lack precision and consistency in the ice studied. Finally, we can also improve the way we heat the sample. In its current state, it is difficult to define the start of the study (during the heating? during the temperature overshoot due to the PID control? or when the target temperature is reached?). Additionally, it is necessary to conduct a series of tests with varying thicknesses and different ice ratios. This will allow for a clearer quantification of the sublimation process within comets.

6.4 Perspective of evolution

In its current state, it is essential to determine whether we are correctly depositing a 3:1 mixture of CO and CO_2. To achieve this, several improvements and additional experiments need to be considered:

- Implementing a more precise control and monitoring system for the deposition process. This could involve using additional sensors to accurately measure the flow rates and quantities of CO and CO_2 being deposited.
- Conducting calibration experiments to verify the accuracy of the deposition system (QMS). These experiments would involve depositing known quantities of CO and CO_2 and comparing the expected ratio with the measured values.

- Enhancing the deposition setup to minimize losses and ensure uniform deposition on the microbalance. This could include optimizing the geometry of the deposition chamber and using more precise pipettes or automated deposition systems.
- Integrating the Low-Energy Electron Diffraction (LEED) technique to confirm the crystallization state of the CO_2. LEED can provide detailed information about the surface structure and ensure that the observed sublimation is due to the intended crystallization process.

We can also try to improve the temperature control system to reduce overshoots and achieve more stable target temperatures. This could involve using more advanced PID controllers and ensuring better thermal contact between the sample and the cryostat.

By addressing these aspects, we can significantly enhance the reliability and accuracy of the experiments, leading to more robust data and better insights into the sublimation and crystallization processes of CO and CO_2. These improvements will not only benefit the current project but also contribute to the broader understanding of sublimation kinetics and crystallization phenomena in planetary science.

7 Conclusion

This internship at NASA, under the California sun and palm trees, was an incredible experience for me. The atmosphere was electrifying, with constant excitement from conferences to the anticipated launch of new missions like Europa Clipper. I chose this internship to test my interest in science, and I came out of it enriched and enlightened.

Even though science is fascinating, I have decided to pursue a career in engineering, specifically through a specialized master's in aerospace at SUPAERO (TAS ASTRO), I know that I will never be far from science. The work being done here has a real impact on the world, from the search for life to the transcendence of human capabilities, which is a true calling for me.

This internship represents a culmination of my engineering degree, confirming that space is the field in which I want to develop my career. The blend of science and engineering at NASA has reinforced my passion and commitment to contributing to the advancements in space exploration. I am deeply grateful for this opportunity, and it has solidified my desire to be part of this industry.

Glossary

AES Auger electron spectroscopy. 8, 10–12, 34

ASI Italian Space Agency. 6

Caltech California Institute of Technology. 5

ESA European Space Agency. 3, 6, 7, 13

FTIR Fourier-transform infrared spectroscopy. 3, 4, 18–22, 24, 26–28, 34

IR Infrared. 8, 19, 20

JMAK Johnson-Mehl-Avrami-Kolmogorov profile. 23

JPL Jet Propulsion Laboratory. 2–8, 13, 34

KBOs Kuiper belt objects. 8

KOALA Quartz crystal microbalance setup. 4, 14–16, 18, 34

LEED Low-Energy Electron Diffraction. 3, 4, 8, 9, 11, 12, 28, 29, 34

LEFTY Infrared spectroscopy setup. 4, 18, 19, 34

MOXIE Mars Oxygen In-Situ Resource Utilization Experiment. 6

MSR Mars Sample Return. 7

NASA National Aeronautics and Space Administration. 2–7, 30

OCIVM OCI Vacuum Microengineering, Inc.. 11

PID Proportional, Integral, Derivative controller. 28, 29

QCM Quartz crystal microbalance. 3, 4, 15, 16

QMS Quadrupole mass spectrometer. 15–18, 28, 34

SHERLOK Scanning Habitable Environments with Raman and Luminescence for Organics and Chemicals. 6

TPD Temperature programmed desorption. 18, 28

WAC Corporal Experimental rocket. 5

References

Gary Attard and Colin Barnes. *Surface*. Oxford University Press, 2011.

M. Avrami. Kinetics of phase change. ii transformation-time relations for random distribution of nuclei. *The Journal of Chemical Physics*, 8(2):212–224, 1940.

Jodi R. Berdis, James R. Murphy, and Nancy J. Chanover. Europa's surface water-ice crystallinity and correlations between linae and hydrate composition. *The Planetary Science journal*, 36, 2022.

D. Bockelee-Morvan, J. Crovisier, M. J. Mumma, and H. A. Weaver. The composition of cometary volatiles. *Comets II*, pages 391–423, 2004.

M. E. Brown. The composition of kuiper belt objects. *California Institute of Technology Press*, 2012.

Brandy Carr, April Evers, Marc Weimer, Brian Smith, and Jeff Leith. Minimizing the outgassing of spin-coated organic materials to reduce defects. *Brewerscience*, 2006.

P. A. Gerakines, W. A. Schutte, J. M. Greenberg, and E. F. van Dishoeck. The infrared band strengths of h2o, co and co2 in laboratory simulations of astrophysical ice mixtures. *Cornell University*, 1994.

P. R. Griffiths and J. A. de Haseth. *Fourier Transform Infrared Spectrometry*. John Wiley & Sons, 2007.

Wolgang hage, Andreas Hallbrucker, Erwin Mayer, and G. P. Johari. Crystallisation kinetics of water below 150k. *The journal of Chemical Physics*, 1993.

David C. Howell. *Statistical Methods for Psychology, Seventh Edition*. Wadsworth Cengage Learning, 2010.

JPL. When computers were human, a. URL `https://www.jpl.nasa.gov/edu/news/2016/10/31/when-computers-were-human/`.

JPL. 7 things to know about the mars 2020 perseverance rover mission, b. URL `https://www.nasa.gov/centers-and-facilities/jpl/7-things-to-know-about-the-mars-2020-perseverance-rover-mission/`.

Youngui Liao. *Practical electron microscopy and database*. Northwestern University, 2006.

Yan Luo, Xiaobin Wu, Kuibo Wang, and Yu Wang. *Comparative Study on the Outgassing Rate of Materials Using Different Methods*. Springer, 2016.

Jeffrey G. Mangum and Yancy L. Shirley. How to calculate molecular column density. *Astronomical Society of the Pacific*, 2015.

Donald A. McQuarrie and John D. Simon. *Physical Chemistry: A Molecular Approach*. University Science Books, 1997.

Mathijs Mutsaers. Zika vector control: Near infrared spectroscopy predicting wolbachia infection in post-mortem aedes aegypti. *Tropical Infectious Diseases, LATHEMA - Fiocruz Institute*, 2018.

NASA. Overview. URL https://science.nasa.gov/mission/voyager/mission-overview/.

B. B. Rath. Kinetics of nucleation and growth processes. *Materials Science and Engineering: B*, 32:101–106, 1995.

T. L. Roush. Physical state of ices in the outer solar system. *Journal of geophysical research*, 106(12):315–323, 2001.

G. Sauerbrey. Verwendung von schwingquarzen zur wägung dünner schichten und zur mikrowägung. *Zeitschrift für Physik*, 155(2):206–222, 1959.

B. Schmitt, S. Espinasse, R. J. A. grim, J. M. Greenberg, and J. Klinger. Laboratory studies of cometary ice analogs. *ESA, Physics and mechanics of cometary materials*, 1989.

B. C. Smith. *Infrared Spectral Interpretation: A Systematic Approach*. CRC Press, 2011.

Sawit Na Songkhla and Takamichi Nakamoto. Overview of quartz crystal microbalance behavior analysis and measurement. *Chemosensors*, 2021.

Nasa Spaceplace. What is a comet. URL https://spaceplace.nasa.gov/comets/en/.

N. Watanabe and A. Kouchi. Ice surface reactions: A key to chemical evolution in space. *Progress in Surface Science*, 83(10):439–489, 2008.

Wikipedia. Cassini-huygens, a. URL https://en.wikipedia.org/wiki/Cassini%E2%80%93Huygens.

Wikipedia. Rosetta(spacecraft), b. URL https://en.wikipedia.org/wiki/Rosetta_%28spacecraft%29#.

List of Figures

8 Appendix

Figure 28: Europa Clipper

Figure 29: CADRE prototype